electronics

MDPI

Article

Calculation of Distribution Network PV Hosting Capacity Considering Source–Load Uncertainty and Active Management

Tingting Lin [1,2], Guilian Wu [1,2,3], Sudan Lai [1,2], Hao Hu [4,*] and Zhijian Hu [4]

[1] Economic and Technological Research Institute, State Grid Fujian Electric Power Co., Ltd., Fuzhou 350013, China; lin_tingting1@fj.sgcc.com.cn (T.L.)
[2] Distribution Network Planning and Operation Control Technology in Multiple Disaster Superimposed Areas State Grid Corporation Laboratory, Ltd., Fuzhou 350013, China
[3] School of Electronic Information and Electrical Engineering, Shanghai Jiao Tong University, Shanghai 200240, China
[4] School of Electrical Engineering and Automation, Wuhan University, Wuhan 430072, China; zj.hu@whu.edu.cn
* Correspondence: hu_hao@whu.edu.cn

Abstract: The access of a high proportion of photovoltaic (PV) will change the energy structure of the distribution network (DN), resulting in a series of safety operation risks. This paper proposes a two-stage PV hosting capacity (PVHC) calculation model to assess the maximum PVHC, considering the uncertainty and active management (AM). Firstly, we employ a robust optimization model to characterize the uncertainty of sources and loads in DN with PV and analyze the worst-case scenarios for PVHC. Subsequently, we construct a PVHC calculation model that takes into account AM, and convert the model into a mixed-integer second-order cone (MISOC) model using linearization techniques. Finally, we apply "heuristic optimization + CPLEX solver" to solve the model and introduce overvoltage and overcurrent indices to analyze the safety of the DN under PV limit access. Case studies are carried out on the IEEE 33-bus system and a practical case. Results show that (1) only the uncertainty that reduces the load or increases the output efficiency will affect PVHC; (2) for DN limited by overvoltage, AM can better improve PVHC; however, for DN limited by maximum transmission power, the effect of AM is low; (3) for most DN, SVC can improve PVHC, but the effect is modest. And network reconfiguration can significantly increase PVHC on the system with poor branch network, even reaching 150% of the original PVHC.

Keywords: distribution network; photovoltaic hosting capacity; source–load uncertainty; active management

Citation: Lin, T.; Wu, G.; Lai, S.; Hu, H.; Hu, Z. Calculation of Distribution Network PV Hosting Capacity Considering Source–Load Uncertainty and Active Management. *Electronics* **2024**, *13*, 4048. https://doi.org/10.3390/electronics13204048

Academic Editor: Ahmed Abu-Siada

Received: 8 September 2024
Revised: 9 October 2024
Accepted: 10 October 2024
Published: 15 October 2024

1. Introduction

1.1. Background

With the depletion of fossil energy such as oil and coal, energy crisis and energy pollution are approaching. According to the International Energy Agency, the new installed capacity of renewable energy in the world reached 510 GW in 2023. China's national energy administration has reported that China's new installed power generation capacity was about 290 GW in 2023. China's installed capacity of renewable energy has surpassed that of thermal power for the first time. As an important renewable energy source, the installed capacity of photovoltaic (PV) accounts for a large proportion of renewable energy. In 2023, the global new installed capacity of PV was 375 GW, accounting for 75% of all the new installed capacity of renewable energy. The rapid development of PV has led to an increasing penetration rate in the distribution network (DN). It is important to consider the maximum PV hosting capacity (PVHC).

Compared with conventional generators, PV is affected by lighting conditions and has great uncertainty. Additionally, the transportation and installation processes of PV systems

can result in losses, further causing the actual output to deviate from the ideal output [1]. The uncertainty caused by the high proportion of PV access will cause a non-negligible impact on DN. In addition, the load of DN also has uncertainty, and its uncertainty cannot be ignored. Therefore, it is necessary to consider the uncertainty of PV and load and to obtain the most unfavorable operation scenario for the maximum PV access to the DN.

In addition, the high proportion of PV access will also change the energy consumption structure of the traditional DN. The energy consumption structure of the traditional DN is to supply power to the DN through the superior grid, so as to meet the electricity demand of DN. When the PV is large enough, the electricity load of the DN will be entirely borne by the PV, and the excess PV power generation will flow to the superior grid, causing the occurrence of the reverse transmission phenomenon (RTP) [2,3]. Figure 1 shows the energy flow of the traditional DN and the DN with a high proportion of PV access. Squares represent balance buses, circles are load buses, triangles are PV grid-connected buses, and arrows indicate the direction of energy flow. It can be seen that the energy of the traditional DN flows from the balancing bus to the remaining load buses. However, the energy flow direction of the DN with a high proportion of PV access is from the PV buses to the rest of the load buses and the balance bus, so its voltage will be higher than the reference voltage at the balance bus [4], which makes the DN have the risk of overvoltage [5,6]. Therefore, although PV has been developed very rapidly due to its environmental protection and renewability, its uncertainty and impact on the security of the DN limit its HC [7,8]. The above analysis shows the adverse factors that affect the PVHC. But, with the development and construction of the intelligent DN, various active management (AM) strategies can effectively improve PVHC, such as network reconfiguration and static Var compensator (SVC) control [9].

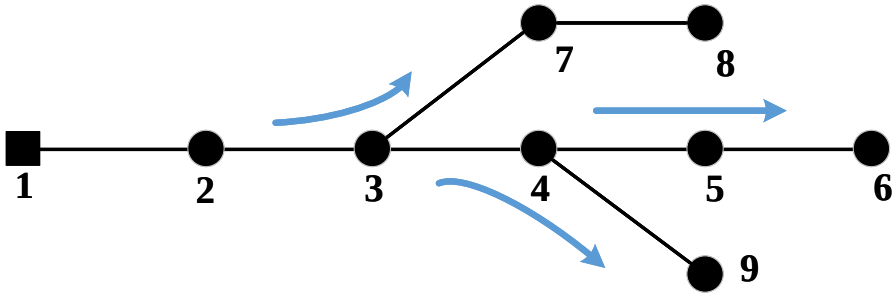

(**a**)

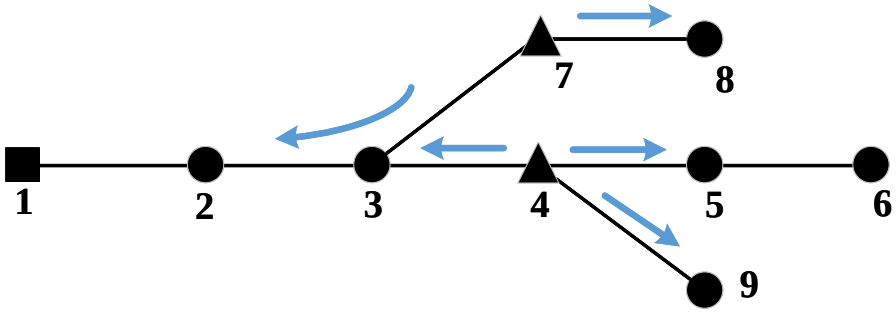

(**b**)

Figure 1. The energy flow direction of DN. (**a**) The traditional DN. (**b**) The DN with a high proportion of PV access.

In summary, the PVHC calculation problem needs to maximize the PVHC using AM while fully considering the DN security and source–load uncertainty.

1.2. Literature Review

PVHC is defined as the maximum installed PV capacity of the DN that does not violate the constraints for the safe operation of the power grid [10]. At present, many scholars have carried out research on the evaluation and calculation of PVHC.

On the evaluation of PVHC, ref. [11] has integrated the impact of distributed generation and new load access on the distribution network, and then established evaluation indexes from five aspects of the distribution network: reliability, safety, economy, flexibility, and quality. The evaluation index of the HC was constructed from the perspectives of power grid architecture and operation state in ref. [12], and the HC was improved through the expansion planning of the DN. On the basis of constructing the HC index, ref. [13] has studied the effect of energy storage and adjusting the transformer tap on the improvement of the HC. The aforementioned literature has assessed PVHC by constructing indicators, yet it has not actually calculated the PVHC itself.

On the calculation of PVHC, ref. [14] has used ETAP simulation software (version: 16.0) to calculate the power flow of the DN that contains PV power sources, under the condition that the power grid voltage constraints and line power flow constraints are met, and combined this with the actual load curve of a certain region, so as to obtain the maximum PVHC that can be connected to the PV power sources. Based on voltage sensitivity and multi-scenario power flow simulation, ref. [15] has proposed a PV acceptance ability evaluation method, which can uniformly generate the possible access scheme of PV and simulates the multi-power flow. In ref. [16], the voltage deviation index and reverse power transmission of high-proportion PV DN were introduced to judge the rationality of the optimization scheme and feed back to the modification layer of the access scheme; then, the calculation results of the PVHC were obtained. In ref. [17], the evaluation system of renewable energy hosting capacity index and the hosting capacity calculation model of the power grid were established after fully considering the power quality, relay protection, and thermal stability test. The particle swarm optimization (PSO) algorithm was used to solve the hosting capacity model. Although the aforementioned literature has calculated PVHC, it is based on deterministic data and does not account for the uncertainty of PV and load within the DN.

It is important to consider the uncertainty of DN when calculating the PVHC. Ref. [18] has used a weighted K-means algorithm to cluster the historical data of distributed PV output to obtain typical scenario data. In refs. [19,20], Monte Carlo simulations were used to counter the uncertainties and variability related to loading behavior and the randomness in the location and size of PV. Considering the uncertainty of PV and load, the scenario of minimum load and maximum PV is finally selected as the worst scenario to calculate the PVHC. Ref. [21] has established a model with high temporal resolution to simulate all the scenarios. Based on the results of the scenarios with different PV power rates and storage capacities, the worst scenario is the scenario with maximum PV power rates and minimum storage capacities. A multi-time scale optimization model is established in Ref. [22], considering the uncertainty of source and load, to realize the calculation of PVHC.

After calculating the PVHC, AM can be taken to improve its HC [23]. In ref. [24], the best number, location, and size of PV systems to be installed on a distribution feeder and the control set-points of the PV inverters were determined to maximize the PVHC. Genetic algorithm (GA) and PSO metaheuristics were employed to solve the optimization problem. In ref. [25], network reconfiguration was studied in a multi-objective framework to improve the voltage profile and decrease the total energy loss, as well as to improve the PVHC. A solution strategy is proposed for the presented multi-objective problem based on the implementation of the Non-dominated Sorting Genetic Algorithm II (NSGA-II) and fuzzy decision-making method. Ref. [26] was devoted to a new multi-objective formulation to maximize the PVHC and minimize the total energy losses while satisfying the operational constraints and maximizing the energy transferred to off-peak hours. The Multi-Objective Advanced Gray Wolf Optimization (MOAGWO) algorithm was used as a solution tool. For fully exploiting the ability of DNs to accommodate PV, ref. [27] proposed a robust comprehensive PVHC assessment method, considering three-phase power flow modelling

and AM techniques, including network reconfiguration, on-load-tap-changers regulation (OLTC), and reactive power compensation. Ref. [28] has proposed a two-stage model, in which the dispatching of soft open point (SOP) and management of electric vehicles (EVs) were coordinated together with traditional AM techniques. A solving strategy based on the column-and-constraint generation (C&CG) algorithm is developed to solve the model.

1.3. Contributions

The above literature studied PVHC from the perspectives of evaluation, calculation, and improvement. This paper focuses on the calculation of PVHC to construct an accurate PVHC calculation model. Noting that most of the calculation models directly make the maximum PVHC the objective, but few of them have considered whether the objective remains the fit for the model after the changes when it was linearized, this paper has proposed a relaxation formula to verify the correctness of the objective. In addition, considering that the PV has its own inverter and the DN has its own backup branch, any DN can take SVC and network reconfiguration to improve the PVHC. Thus, it is necessary to consider the SVC and network reconfiguration when constructing the PVHC calculation model.

In this paper, a PVHC calculation model and improvement method considering the uncertainty of DN has been proposed. The source–load uncertainty is described by robust optimization. Meanwhile, the PVHC calculation model is constructed under the constraints of DN safety and practical, PV configuration, RTP, and AM methods, and then linearized to a mixed-integer second-order cone (MISOC) model. The validity of the objective is verified by the relaxation verification formula, and the safety of DN operation is verified by the overvoltage margin and overcurrent margin indexes. Table 1 compares the proposed model of this paper with the relevant research on PVHC recently.

Table 1. Comparison of the relevant research.

Ref.	Uncertainty Analysis	Model Solution	PVHC Improvement	Model Evaluation
[17]	None	PSO	Energy storage	None
[20]	Monte carlo simulation	Traversal algorithm	None	Overvoltage limit violation, equipment ampacity violation
[21]	Stochastic simulation	High temporal resolution simulation	Distributed storage	Demand cover factor, supply cover factor, grid interaction supply cover factor, exported energy factor
[22]	Monte carlo simulation	MATLAB optimization toolbox	None	Line capacity, node overvoltage, net load deviation
[24]	None	GA and PSO	SVC	None
[25]	Probabilistic assessments	NSGA-II	Network reconfiguration	Fuzzy decision-making
[26]	None	MOAGWO algorithm	Energy storage, OLTC, SVC	None
[27]	Robust optimization	C&CG algorithm	network reconfiguration, OLTC, reactive power compensation	None
[28]	Robust optimization	C&CG algorithm	EV management, SOP, network reconfiguration, OLTC, reactive power compensation	None
This paper	Robust optimization	Traversal algorithm, CPLEX	Network reconfiguration, SVC	Relaxation deviation, overvoltage margin, overcurrent margin

From the above, the key contributions of this study are listed below:

(1) An MISOC model was established to calculate and improve the PVHC. Unlike other papers, we propose a relaxation verification formula to assess the relaxation validity of the MISOC model;
(2) To evaluate the safety of the DN under PV limit access, the overvoltage and overcurrent margin indexes are set. The effects of maximum current, maximum voltage, maximum reverse transmission, and PV inversion angle on PVHC are analyzed by sensitivity analysis;
(3) To analyze the enhancement effect of the AM method on PVHC, we applied an AM method to three kinds of DN systems that are susceptible to transmission power, current, or voltage.

The remainder of this paper is organized as follows. In Section 2, a source–load uncertainty model is constructed based on robust optimization, then the worst scenario is obtained through PVHC analysis. Section 3 constructs a two-stage MISOC calculation model considering safety constraints and AM methods. In Section 4, a solution framework based on heuristic optimization and solver is elaborated. In Section 5, the proposed model is demonstrated, analyzed, and discussed on the IEEE 33-bus system and a practical case in Fuzhou, Fujian. And conclusions are provided in Section 6.

2. The Worst Scenario Considering Source–Load Uncertainty

2.1. Source–Load Uncertainty Analysis

The DN with PV access receives or transmits power to the higher power grid through the transmission line; the main power generation source is PV, and the power consumption sources are load and network loss, as shown in Figure 2. Among these, PV and load have uncertainty [29,30]. Robust optimization ensures that, even in the worst scenario, the optimization solution is feasible [31]. Refs. [32,33] established an adaptive robust stochastic optimization model to address the renewable power uncertainty modeled as a scenario-based ambiguity set. We describe the uncertainty of PV and load by this method. Furthermore, considering the absolute nature of PVHC, any solution within the uncertainty set should yield a value greater than the resulting PVHC. Therefore, the key to solving this uncertainty problem lies in identifying the worst-case scenario for PVHC calculation. As in (1)–(3), we describe the source–load uncertainty through box uncertainty sets.

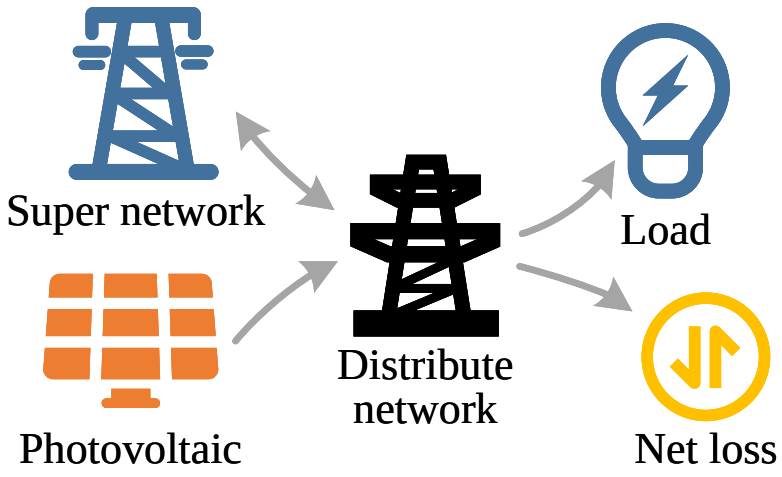

Figure 2. DN source–load balance.

$$\varphi_{v,s} = \varphi'_{v,s} + \alpha_{v+,s}\Delta\varphi_{v+,s} - \alpha_{v-,s}\Delta\varphi_{v-,s} \tag{1}$$

$$P_{v,i,s} = \varphi_{v,s}S_{v,i,s} \tag{2}$$

$$P_{d,i,s} = P'_{d,i,s} + \alpha_{d+,i,s}\Delta P_{d+,i,s} - \alpha_{d-,i,s}\Delta P_{d-,i,s} \tag{3}$$

where $\varphi_{v,s}$, $\varphi'_{v,s}$, $\Delta\varphi_{v+,s}$, and $\Delta\varphi_{v-,s}$ are the actual, prediction, upward deviation, and downward deviation of PV power generation efficiency in scenario s; the box uncertainty set of $\varphi_{v,s}$ is $[\varphi'_{v,s} - \Delta\varphi_{v-,s}, \varphi'_{v,s} + \Delta\varphi_{v+,s}]$; $P_{d,i,s}$, $P'_{d,i,s}$, $\Delta P_{d+,i,s}$, and $\Delta P_{d-,i,s}$ are the actual, prediction, upward deviation, and downward deviation of load in scenario s and bus i; the box uncertainty set of $P_{d,i,s}$ is $[P'_{d,i,s} - \Delta P_{d-,i,s}, P'_{d,i,s} + \Delta P_{d+,i,s}]$; $\alpha_{v+,s}$, $\alpha_{v-,s}$, $\alpha_{d+,i,s}$, and $\alpha_{d-,i,s}$ are the source–load uncertainty deviation coefficients, which have values between 0 and 1; and $P_{v,i,s}$, $S_{v,i,s}$ are the PV power generation and configured capacity in scenario s and bus i.

2.2. PVHC Analysis

Equation (4) represents that PV output of each scenario that can be obtained based on power balance. Without considering the abandonment of PV output, the output of PVHC should always not exceed the PV output of each scene, as in (5).

$$P_{v,s} = P_{d,s} + P_{loss,s} + P_{up,s} \tag{4}$$

$$S_v \leq \frac{1}{\varphi_{v,s}}(P_{d,s} + P_{loss,s} + P_{up,s}) \tag{5}$$

where $P_{v,s}$, $P_{d,s}$, and $P_{loss,s}$ are the DN's total PV generation, load, and loss in scenario s; $P_{up,s}$ is the power transmission from the DN to the upper power network in scenario s. S_v is the PVHC of DN.

From Equation (5), we can see that, the bigger the value of $\varphi_{v,s}$ is and the smaller the values of $P_{d,s}$ and $P_{up,s}$, the worse the scenario. In ref. [19,34], it is also proven that the worst scenario is the lowest load and the highest PV output through Monte Carlo simulations. Therefore, the uncertain scenario with the largest $P_{d,s}$ and the smallest $\varphi_{v,s}$ should be selected, as in (6) and (7).

$$\varphi_{vmax,s} = \varphi'_{v,s} + \Delta\varphi_{v+,s} \tag{6}$$

$$P_{dmin,i,s} = P'_{d,i,s} - \Delta P_{d-,i,s} \tag{7}$$

where $\varphi_{vmax,s}$ and $P_{dmin,i,s}$ are the maximum PV power generation efficiency and the minimum load.

3. Problem Description

The PVHC calculation problem proposed in this paper aims to find out where to configure the PV and how much capacity of PV to configure in order to realize the maximum PV capacity of the DN in scenarios, while making sure to fulfill many DN operation and safety constraints, while also embracing the many constraints of the AM methods.

3.1. Problem Formulation

3.1.1. Objective Function

The objective function of PVHC estimation maximizes the capacity of PV that can be installed for all buses. This can be expressed as follows:

$$maxS_{v,s} = \sum_{i=1}^{n_b} S_{v,i,s} \tag{8}$$

where n_b is the total number of buses.

3.1.2. DN Power Flow Constraints

In this part, power balance constraints, voltage balance constraints [35], and complex power constraints are considered [36], as shown in (9)–(12).

$$\begin{cases} P_{v,i,s} - P_{d,i,s} = \sum\limits_{j \in \Omega_{up,i}} P_{j,s} - \sum\limits_{j \in \Omega_{down,i}} (P_{j,s} - r_j I_{j,s}^2) \\ Q_{v,i,s} - Q_{d,i,s} = \sum\limits_{j \in \Omega_{up,i}} Q_{j,s} - \sum\limits_{j \in \Omega_{down,i}} (Q_{j,s} - x_j I_{j,s}^2) \end{cases} \tag{9}$$

$$\begin{cases} -P_{up,s} = \sum\limits_{j \in \Omega_{up,i}} P_{j,s} - \sum\limits_{j \in \Omega_{down,i}} (P_{j,s} - r_j I_{j,s}^2) \\ -Q_{up,s} = \sum\limits_{j \in \Omega_{up,i}} Q_{j,s} - \sum\limits_{j \in \Omega_{down,i}} (Q_{j,s} - x_j I_{j,s}^2) \end{cases} \tag{10}$$

$$V_{i2,s}^2 = V_{i1,s}^2 - 2(r_j P_{j,s} + x_j Q_{j,s}) + (r_j^2 + x_j^2) I_{j,s}^2 \tag{11}$$

$$I_{j,s}^2 V_{i1,s}^2 = P_{j,s}^2 + Q_{j,s}^2 \tag{12}$$

where $P_{j,s}$, $Q_{j,s}$, and $I_{j,s}$ are the active power, reactive power, and branch current in scenario s and branch j; r_j and x_j are the resistance and reactance of branch j; $Q_{v,i,s}$, $Q_{d,i,s}$ are the reactive PV power and reactive load in scenario s and bus i; $Q_{up,s}$ is the reactive power transmission from the DN to the upper power network in scenario s; $\Omega_{up,i}$ and $\Omega_{down,i}$ are the branch set with bus i as the start and end bus; and $V_{i1,s}$ and $V_{i2,s}$ are the start bus and end bus voltage of branch j in scenario s.

3.1.3. DN Safety Constraints

Equation (13) indicates that the voltage of each bus in DN should be within the voltage safety threshold, and Equation (14) indicates that the current of each branch in DN cannot exceed its maximum value [37].

$$V_{min} \le V_{i,s} \le V_{max} \tag{13}$$

$$\left| I_{j,s} \right| \le I_{max} \tag{14}$$

where V_{min} and V_{max} are the minimum and maximum voltage threshold; I_{max} is the maximum current threshold.

3.1.4. RTP Constraints

When the DN supplies or sends power to the upper power network, the maximum transmission power is limited due to the capacity constraint of the transformer [9], as in (15).

$$P_{up,s} \le P_{up,max} \tag{15}$$

where $P_{up,max}$ are the maximum transmission power threshold.

3.1.5. PV Configuration Constraints

For PV buses, the configured capacity should be within the capacity threshold, as in (16). The PV reactive power output is obtained by (17). If SVC is not considered, $\theta_{v,i,s}$ is set to a fixed value. Otherwise, $\theta_{v,i,s}$ can be set within a certain range, as in (18).

$$S_{v,min} \le S_{v,i,s} \le S_{v,max} \tag{16}$$

$$Q_{v,i,s} = P_{v,i,s} tan\theta_{v,i,s} \tag{17}$$

$$-\theta_{v,max} \le \theta_{v,i,s} \le \theta_{v,max} \tag{18}$$

where $S_{v,min}$ and $S_{v,max}$ are the minimum and maximum PV configuration capacity; $\theta_{v,i,s}$ is the inverse angle of scenario s and bus i; $\theta_{v,max}$ is the maximum inverse angle.

3.1.6. Network Reconfiguration Constraints

During the planning phase, the DN adopts a closed-loop design, whereas, during actual operation, it needs to maintain an open-loop configuration. Consequently, backup lines are available, making network reconfiguration feasible. Furthermore, since the original DN topology design did not take into account the scenario of PV limit access, it is of great significance to explore the optimal topology for PVHC through network reconfiguration. The topology of the reconfigured DN must meet the radiation and connectivity constraints [9,38].

$$\sum_{j\in\Omega_{down,i}} F_{j,s} - \sum_{j\in\Omega_{up,i}} F_{j,s} = 1 \tag{19}$$

$$\sum_{j\in\Omega_{up,1}} F_{j,s} = \varepsilon_g \tag{20}$$

$$\sum_{j=1}^{n_l} F_{j,s} = n_b - 1 \tag{21}$$

$$P_{j,s} = 0, Q_{j,s} = 0, I_{j,s} = 0, F_{j,s} = 0, if\ \alpha_{j,s} = 0 \tag{22}$$

where $\alpha_{j,s}$ and $F_{j,s}$ are the branch switch status and virtual power of scenario s and branch j; ε_g is an arbitrary number.

3.2. Linearization Analysis

There are nonlinear constraints in the constructed calculation model, which needs to be linearized [39]. Introduce a quadratic variable $I_{j,s}^2/V_{i,s}^2$ instead of $I_{2,j,s}/\ V_{2,i,s}$ to eliminate the current and voltage squared terms, as in (23)–(26). When network reconfiguration is considered in the model, all the parameters of the disconnected line are 0. The large M method is introduced to linearize the above conditional constraints, as in (27) and (28).

$$\begin{cases} P_{v,i,s} - P_{d,i,s} = \sum\limits_{j\in\Omega_{up,i}} P_{j,s} - \sum\limits_{j\in\Omega_{down,i}} (P_{j,s} - r_j I_{2,j,s}) \\ Q_{v,i,s} - Q_{d,i,s} = \sum\limits_{j\in\Omega_{up,i}} Q_{j,s} - \sum\limits_{j\in\Omega_{down,i}} (Q_{j,s} - x_j I_{2,j,s}) \end{cases} \tag{23}$$

$$\begin{cases} -P_{up,s} = \sum\limits_{j\in\Omega_{up,i}} P_{j,s} - \sum\limits_{j\in\Omega_{down,i}} (P_{j,s} - r_j I_{2,j,s}) \\ -Q_{up,s} = \sum\limits_{j\in\Omega_{up,i}} Q_{j,s} - \sum\limits_{j\in\Omega_{down,i}} (Q_{j,s} - x_j I_{2,j,s}) \end{cases} \tag{24}$$

$$V_{min}^2 \le V_{2,i,s} \le V_{max}^2 \tag{25}$$

$$I_{2,j,s} \le I_{max}^2 \tag{26}$$

$$-M\alpha_{j,s} \le V_{2,i2,s} - V_{2,i1,s} + 2(r_j P_{j,s} + x_j Q_{j,s}) - (r_j^2 + x_j^2) I_{2,j,s} \le M\alpha_{j,s} \tag{27}$$

$$-M\alpha_{j,s} \le P_{j,s}, Q_{j,s}, I_{2,j,s}, F_{j,s} \le M\alpha_{j,s} \tag{28}$$

where $V_{2,i,s}$ and $I_{2,j,s}$ are the square of voltage and current; M is a maximal positive value.

Equation (12) is transformed into a second-order cone form and treated with relaxation [40], as in (29).

$$\left\| \left[2P_{j,s}, 2Q_{j,s}, I_{2,j,s} - V_{2,i1,s} \right]^T \right\|_2 \le I_{2,j,s} + V_{2,i1,s} \tag{29}$$

When linearizing Equation (12), relaxation is carried out, so it is necessary to verify whether the solution results still satisfy the original constraints, as in (30).

$$\sum_{j=1}^{n_l} (I_{2,j,s} V_{2,i1,s} - P_{j,s}^2 - Q_{j,s}^2)^2 \le \varepsilon_{min} \tag{30}$$

where ε_{min} is a minimal positive value close to zero.

When the model is verified by (30), it is found that the error is much larger than 0 when Equation (8) is used as the objective function, indicating that Equation (8) cannot be relaxed under this objective function and the objective function needs to be adjusted. When the objective function is adjusted to verify the effectiveness of second-order cone relaxation, it is found that the relaxation results satisfy the original constraints when the loss of the network is reduced by the objective function. Based on the above analysis, the model is adjusted to a two-stage MISOC model with the maximum PVHC in the first stage and the minimum network loss in the second stage, as in (31).

$$\begin{cases} \max S_{v,s} \\ \begin{cases} \min P_{loss,s} = \sum_{j=1}^{n_l} I_{2,j,s} r_j \\ s.t.\ (15\text{–}21), (23\text{–}29) \end{cases} \end{cases} \tag{31}$$

4. Solution Methodology

The model is divided into two stages. The first stage is the outer max problem, which maximizes the PVHC. The second stage is the inner layer min problem, which determines the PV configuration plan, the switch status of each branch, and the power angle of the inverter to minimize the network loss. To solve this problem, the method of "variable step size traversal + solver" is adopted, as in Figure 3.

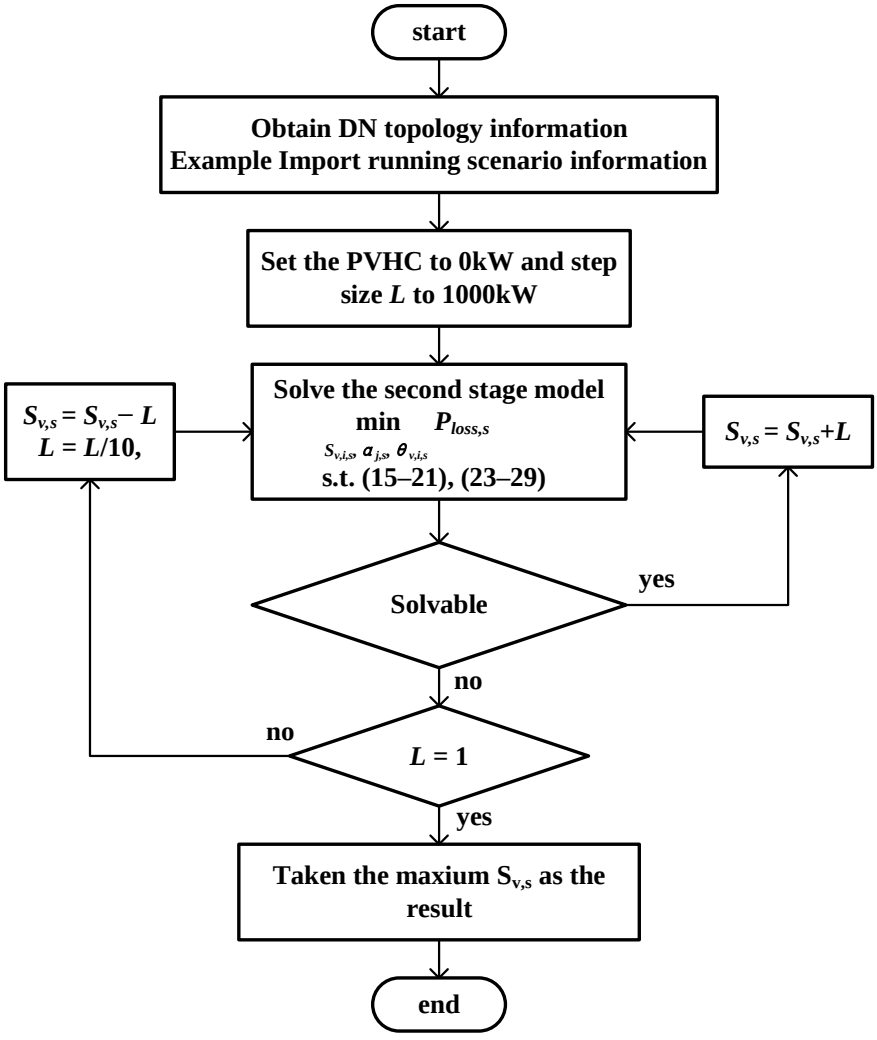

Figure 3. PVHC model solving strategy.

The specific solution strategy is as follows:

(1) Input PV output efficiency and load data to obtain the model calculation scenario;
(2) Set the PVHC to 0 kW and the initial step size to 1000 kW;
(3) Put it into the second stage model, solve the model, and obtain the PV configuration plan and the switch state of each branch;
(4) Judge the safety of the result and calculate the overvoltage margin and overcurrent margin, as in (32) and (33).

$$V_{out,s} = \frac{V_{max} - max(V_{i,s})}{V_{max}} \tag{32}$$

$$I_{out,s} = \frac{I_{max} - max(I_{j,s})}{I_{max}} \tag{33}$$

where $V_{out,s}$ and $I_{out,s}$ are the overvoltage and overcurrent margin;
(5) If the result does not exceed the safety limit and meets Equation (30), increase the PVHC by a step and return to step 3;
(6) If the result makes the overvoltage or overcurrent not satisfy Equation (30) and if the step is longer than 1, return to the previous PVHC and reduce the step size to one-tenth of the original, then return to step 3. If the step length is 1, the last solution result is output, and the PVHC at this time is the result.

5. Case Studies

The model is analyzed using the IEEE 33-bus system and a DN practical case in Fuzhou, Fujian. The mathematical formulation of the proposed model is programmed in Python 3.6. The solver is CPLEX 12.8. All the simulations are implemented in a Windows 11 environment with Inter (R) Core (TM) i7-13700 CPU (3.40 GHz, 16 GB RAM).

5.1. IEEE 33-Bus System

5.1.1. Data and Result Analysis

The rated capacity of the IEEE 33-bus system is 10 MVA, the rated voltage is 12.66 kV, the voltage threshold is [0.95, 1.05] p.u. (expressed by unit value), and the maximum current is 500 A [39]. The maximum transmission power is 6 MW. The branch and bus data can be found in ref. [41]. Except for the balance bus, the remaining buses can be installed PV generators, and the threshold is [100, 800] kW. ε_{min} is set to 10^{-6}. The load types of buses are shown in Table 2.

According to the impact analysis of PVHC, the moment of output efficiency [1, 0.9, 0.85, 0.8, 0.75] is selected as the scenario for analysis. Moreover, the moment with the smallest load is selected as the load of the scene. Based on the above analysis, we have set five typical scenarios, as shown in Table 3.

Table 2. Bus load type of the IEEE 33-bus system.

Load Type	Buses
Resident	4/7/10/13/16/19/22/25/28/31
Commercial	2/5/8/11/14/17/20/23/26/29/32
Industrial	3/6/9/12/15/18/21/24/27/30/33

Table 3. The bad scenarios of the IEEE 33-bus system.

Scenes	Efficiency	Resident (kW)	Commercial (kW)	Industrial (kW)
1	1	200	160	160
2	0.9	100	130	130
3	0.85	90	140	140
4	0.8	80	160	160
5	0.75	135	140	140

Without considering the uncertainty and AM (the standby branch disconnection and $\theta_{v,i,s}$ are set to 5°), the results of each scenario are shown in Table 4. From the table, we see that scenario 2 has the smallest PVHC. As such, scenario 2 is the worst scenario in DN, and the PVHC of the DN is 11.073 MW. Comparing scenarios 2, 3, and 4, it is found that PVHC increases as the PV output efficiency decreases under similar loads. This indicates that the PV output efficiency of the worst scenario in which PVHC is calculated should be as large as possible. Comparing scenarios 1 and 2, although scenario 2 has a smaller output efficiency, its PVHC is smaller due to its smaller load. This further illustrates that PVHC is proportional to the load size, and the scenarios with smaller loads are closer to the worst scenario.

Table 4. Results of the five typical scenarios.

Scenes	Reverse Power (kW)	PVHC (kWp)	Overvoltage (%)	Overcurrent (%)	Relaxation Deviation
1	6000	11,623	2.29	3.70	10^{-7}
2	6000	11,073	2.17	4.06	10^{-7}
3	6000	11,882	1.81	3.84	10^{-7}
4	5921	12,946	2.01	5.26	10^{-5}
5	5373	13,196	2.28	13.94	10^{-5}

The bus voltages and branch currents of each scenario are shown in Figures 4 and 5. From the figures, it can be found that the voltage is minimum at the balancing bus and gradually increases towards the PV configuration bus, and that the current is maximum at the balancing bus and gradually decreases towards the PV configuration bus. This phenomenon reflects the situation of DN with maximum access to PV. In this case, the RTP that causes the power flow back occurs, making the voltage and current characteristics opposite to the original.

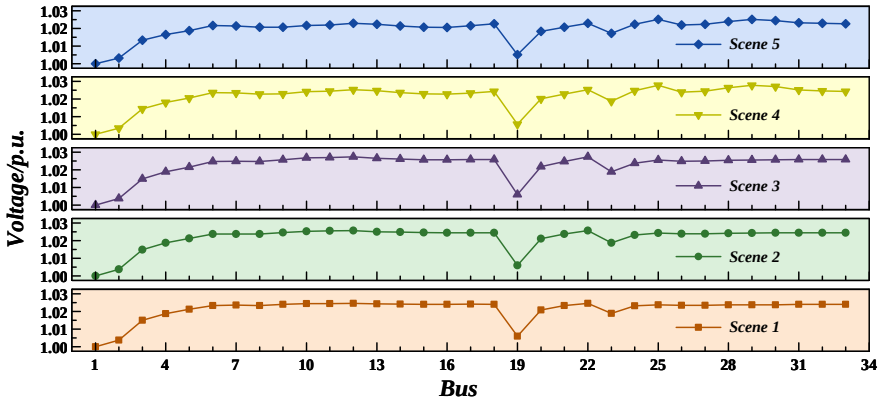

Figure 4. Bus voltage in the five typical scenarios.

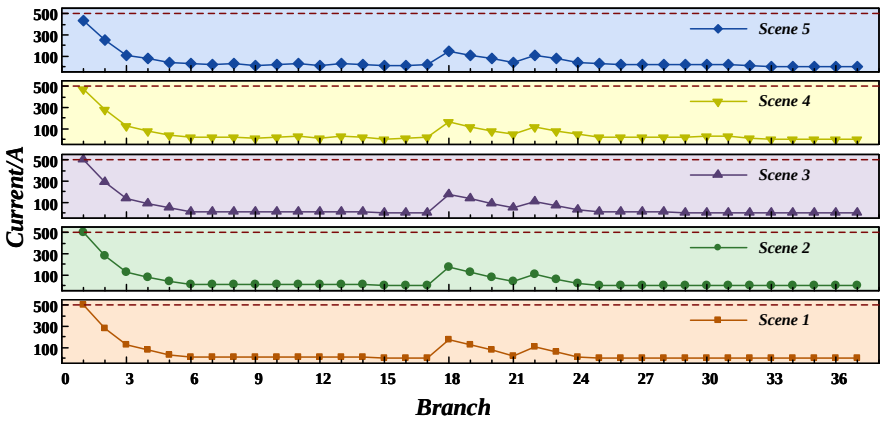

Figure 5. Branch current in the five typical scenarios.

The PV configuration scheme for scenario 2 is shown in Figure 6, and the data format is bus/capacity (kW). Based on the configuration scheme, PV is mainly configured in the buses that are near the balance bus, and only a small amount of PV is configured for other buses. By analyzing the reasons for the above situation, it can be concluded that the strategy of this paper is to first configure PV in each bus to absorb the load, and then configure PV in the bus closer to the balance bus for reverse power supply. This strategy can effectively shorten the power flow and alleviate the rise of voltage and current in the DN.

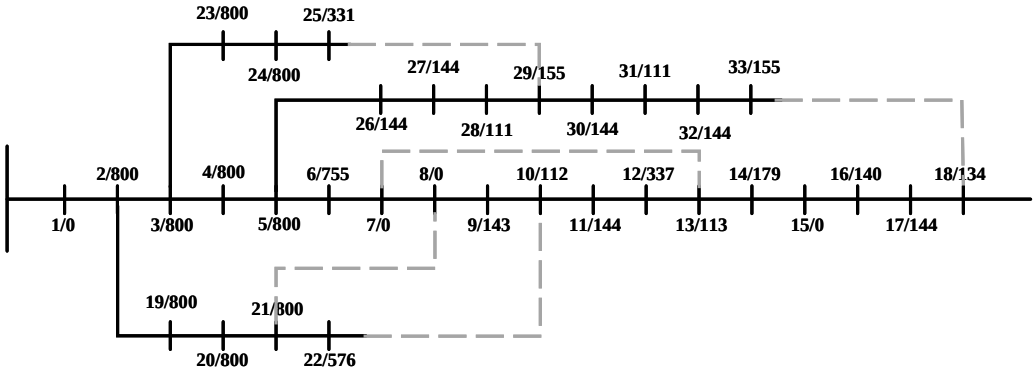

Figure 6. PV configuration scheme in scenario 2.

Taking scenario 2 as the base scenario, the paper analyzes the model validity, uncertainty, sensitivity, and AM method as follows.

5.1.2. The Validity Analysis

We adjust the objective function of the model to the maximum PVHC and the maximum reverse power, and the relaxation deviation of the results are 3.831 and 4.216, respectively. The result shows that second-order cone relaxation cannot be used to linearize the model when the PVHC maximum is the objective function directly. The relaxation deviation of the two-stage model established in this paper is less than 10 with the minimum loss as the objective function. The two-stage model constructed in this paper aims to maximize the PVHC in the first stage and minimize the loss in the second stage. The linearized model is solved in the second stage, and the relaxation deviation is less than 10^{-5}. It shows that the results obtained by the model constructed in this paper still satisfy the original constraints.

5.1.3. The Uncertainty Analysis

This paper has concluded in the result analysis that the worst scenario has larger output efficiency and smaller load. Therefore, only the uncertainty that stems from increasing the output efficiency or decreasing load can make the scenario worse. And the worst uncertainty scenario is the one with maximum output efficiency and minimum load. To prove this conclusion, the output efficiency and load are adjusted respectively for comparative analysis. The results are shown in Figure 7, where the horizontal coordinate represents the adjustment ratio of efficiency or load. From the figure, it can be intuitively seen that PVHC is inversely proportional to efficiency and proportional to load, and efficiency affects PVHC more than load.

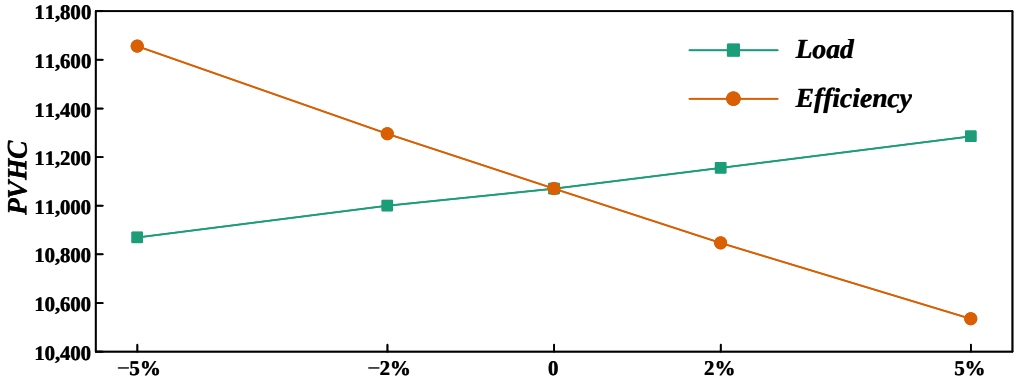

Figure 7. Uncertainty analysis results.

5.1.4. The Sensitivity Analysis

(1) Maximum current.

In scenario 2, we set the maximum current to [300, 400, 500, 600, 700] A, and the calculated results are shown in Table 5. It can be seen that the PVHC increases as the maximum current increases from 300 to 500. But, when the maximum current is from 500 to 700, the PVHC does not increase. This is because PVHC is mainly limited by current risk when the maximum current is low. Therefore, PVHC increases with the increase in the maximum current. But, when the maximum current is high enough, PVHC is mainly limited by the maximum reverse power, so that the PVHC does not increase with the maximum current. After accurate calculation, the critical maximum current of the above two cases is 480 A.

Table 5. Sensitivity analysis results of maximum current.

Current Maximum (A)	Reverse Power (kW)	PVHC (kWp)	Overvoltage (%)	Overcurrent (%)
300	3743	8482	3.63	0
400	4996	9909	3.03	0
500	6000	11,073	2.17	4.06
600	6000	11,073	2.17	20.05
700	6000	11,073	2.17	47.97

(2) Maximum voltage.

We set the maximum voltage to [1.02, 1.03, 1.04, 1.05, 1.06] p.u.; the calculated results are shown in Table 6. When the maximum voltage comparison is small, PVHC will increase with the increase in the maximum voltage. But, when the maximum voltage is large, PVHC does not increase. The critical maximum voltage of the above two cases is 1.0253 p.u..

Table 6. Sensitivity analysis results of maximum voltage.

Maximum Voltage (p.u.)	Reverse Power (kW)	PVHC (kWp)	Overvoltage (%)	Overcurrent (%)
1.02	5312	10,272	0	14.98
1.03	6000	11,073	0.27	4.06
1.04	6000	11,073	1.23	4.06
1.05	6000	11,073	2.17	20.05
1.06	6000	11,073	3.09	47.97

(3) Maximum transmission power.

We set the maximum transmission power to [5, 5.5, 6, 6.5, 7] MW; the calculated results are shown in Table 7. From the table, it can be seen that the PVHC increases with the increase in the maximum transmission power before the critical value. But, when the maximum transmission power reaches 6.256 MW, the overcurrent is 0, and the PVHC will not increase again.

Table 7. Sensitivity analysis results of maximum transmission power.

Maximum Transmission Power (MW)	Reverse Power (MW)	PVHC (kWp)	Overvoltage (%)	Overcurrent (%)
5	5	9915	2.86	19.90
5.5	5.5	10,490	2.71	11.98
6	6	11,073	2.17	4.06
6.5	6.256	11,365	2.18	0
7	6.256	11,365	2.18	0

(4) The inverse angle.

We set $\theta_{v,i,s}$ to [−5, −2, 2, 5] MW; the calculated results are shown in Table 8. From the table, if can be found that the fixed $\theta_{v,i,s}$ has little effect on PVHC. But, when a is close to 0, the current of DN will decrease, which can effectively alleviate the risk of overcurrent.

Table 8. Sensitivity analysis results of the inverse angle.

$\theta_{v,i,s}$	Reverse Power (kW)	PVHC (kWp)	Overvoltage (%)	Overcurrent (%)
−5	6000	11,080	2.67	3.64
−2	6000	11,070	2.58	46.20
2	6000	11,072	2.21	47.80
5	6000	11,073	2.17	4.06

5.1.5. The AM Methods Analysis

We set 3 cases to compare with the original results. Case 1 considers network reconfiguration, and case 2 considers SVC, which can adjust $\theta_{v,i,s}$ between −5° and 5°. Case 3 considers both network reconfiguration and SVC. The results are shown in Table 9. From the table, we can see that the difference between the results that take AM methods and the original results is low. We think that this condition occurs because the PVHC of the original DN system is mainly limited by the maximum transmission power, which cannot be improved by AM methods.

Table 9. The AM methods analysis results of the original DN.

Case	Origin	1	2	3
AM	None	Reconfiguration	SVC	Both
Reverse power (kW)	6000	6000	6000	6000
PVHC (kWp)	11,073	11,067	11,072	11,069
Overvoltage (%)	2.17	2.39	2.24	2.52
Overcurrent (%)	4.06	4.36	4.82	4.80
Off branches	33/34/35/36/37	8/13/25/32/33	33/34/35/36/37	9/25/33/34/36

From the inverse angle sensitivity analysis, we see that SVC can alleviate the risk of overcurrent. To verify this conclusion, we decrease the maximum current to 300 A, which makes the DN more prone to overcurrent risk, and then compare the effects of the AM methods again. The results are shown in Table 10. It can be seen that the SVC increases the PVHC by 45 kW, but the effect of network reconfiguration is still low.

Based on the original system, the maximum voltage is adjusted to 1.02 p.u. The comparison between the results of the AM method and the original results is shown in Table 11. From the table, we can see that both network reconfiguration and SVC can increase the PVHC in the DN that is more prone to overvoltage. And SVC can increase the PVHC by 400 kW, while network reconfiguration increases the PVHC by 60 kW. This means that AM methods are more effective in DN, which is prone to overvoltage.

Table 10. The AM methods analysis results of the overcurrent DN.

Case	Origin	1	2	3
AM	None	Reconfiguration	SVC	Both
Reverse power (kW)	3743	3735	3790	3790
PVHC (kWp)	8482	8471	8527	8529
Overvoltage (%)	3.63	3.60	3.81	3.80
Overcurrent (%)	0	0	0	0
Off branches	33/34/35/36/37	10/14/16/28/33	33/34/35/36/37	6/8/11/12/27

Table 11. The AM methods analysis results of the overvoltage DN.

Case	Origin	1	2	3
AM	None	Reconfiguration	SVC	Both
Reverse power (kW)	5312	5364	5674	5744
PVHC (kWp)	10,272	10,330	10,685	10,766
Overvoltage (%)	0	0	0	0
Overcurrent (%)	14.98	14.48	10.08	8.94
Off branches	33/34/35/36/37	11/14/17/27/33	33/34/35/36/37	6/8/13/26/37

5.2. Practical Case

To further demonstrate the applicability and practicability of the model, the PVHC calculation model is applied in a practical case. As shown in Figure 8, the practical case consists of 17 buses and 20 branches, in which branches 17, 18, 19, 20 are the spare branches. In this system, the output efficiency is 0.9, and the resident, commercial, and industrial loads are 200, 160, and 160 kW. The load type of buses is shown in Table 12, and the branch data are shown in Table 13. The maximum transmission power is 7 MW. The data not mentioned are the same as the IEEE 33-bus system. Four cases are set up according to the type of AM method taken, and the calculation results are shown in Table 14.

From Table 14, it can be seen that the SVC increases the PVHC by 166 kW, which is similar to the results of the IEEE 33-bus system. But network reconfiguration increased the PVHC by 3272 kW, which is much larger than the IEEE 33-bus system. As for the completely different effects of network reconfiguration in the two cases, we think that these are due to the difference in the branch networks of each case. The branch network in the IEEE 33-bus system is superior, so the effect of network reconfiguration on PVHC improvement is small, while the branch network in the practical case is not suitable for the situation of a large number of PV access, so the network reconfiguration can effectively improve PVHC. Based on the above analysis, it can be concluded that SVC can improve the PVHC, but the effect is mediocre. For systems with poor branch networks, network reconfiguration can significantly increase PVHC by more than 50%.

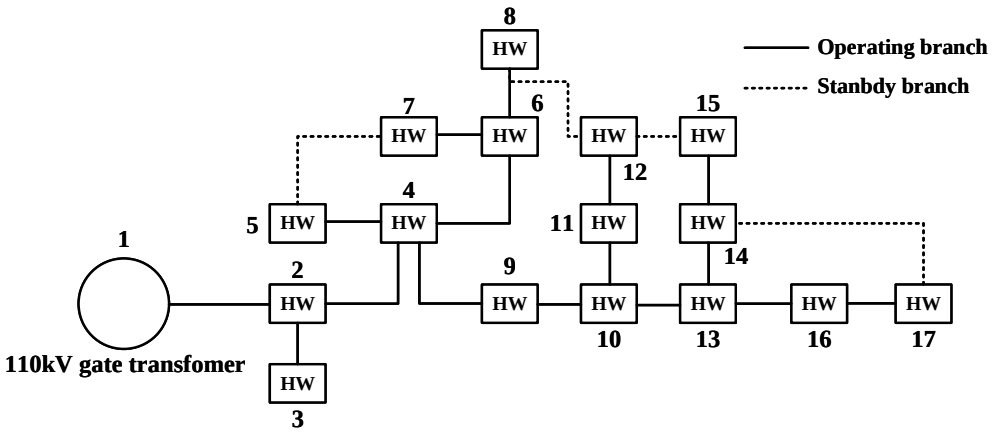

Figure 8. Topology of the practical case.

Table 12. Bus load type in the practical case.

Load Type	Buses
Resident	5/6/12/14/15
Commercial	4/7/9/10/11/13/16/17
Industrial	2/3/8

Table 13. Branch data for the practical case.

Branch	Begin Bus	End Bus	Resistance (Ω)	Reactance (Ω)
1	1	2	0.3431	0.1909
2	2	3	0.2244	0.1249
3	2	4	0.3392	0.1887
4	4	5	0.2494	0.1388
5	4	6	0.3292	0.1832
6	6	7	0.1496	0.0833
7	6	8	0.0948	0.0527
8	4	9	0.3392	0.1887
9	9	10	0.1692	0.0944
10	10	11	0.3611	0.2009
11	11	12	0.1337	0.0744
12	10	13	0.3641	0.2026
13	13	14	0.2244	0.1249
14	14	15	0.3112	0.1732
15	13	16	0.2025	0.1127
16	16	17	0.2753	0.1532
17	5	7	0.3392	0.1887
18	8	12	0.3392	0.1887
19	12	15	0.3392	0.1887
20	14	17	0.3392	0.1887

Table 14. The AM methods analysis results in the practical case.

Case	1	2	3	4
AM	None	Reconfiguration	SVC	Both
Reverse power (kW)	3378	6201	3521	6242
PVHC (kWp)	6873	10,145	7039	10,189
Overvoltage (%)	3.31	1.45	3.34	7.30
Overcurrent (%)	45.62	0	43.96	0
Off branches	17/18/19/20	6/11/13/16	17/18/19/20	6/11/14/15

5.3. Comparison of Solution Methods

The second-order cone relaxation method is adopted in the linearization. If the model is solved directly, the relaxation deviation will be too large, resulting in the original constraint becoming invalid. For this case, ref. [28] reduces the relaxation deviation by iterative approximation. And the method proposed in this paper solves this problem by constructing a two-stage model. In the second stage, the minimum loss is the goal while trying to ensure the effectiveness of second-order cone relaxation, and, in the first stage, the maximum PVHC is the goal while trying to obtain the calculation results. The results of the two methods are listed in Table 15.

In the IEEE 33-bus system, the PVHC obtained by the two methods is almost the same when the AM is not adopted. However, the PVHC obtained in ref. [28] is larger than that in this paper after AM is adopted. The above situation occurs because the method in this paper limits the loss. Therefore, different from ref. [28], the method in this paper does not increase the PVHC by increasing the loss. In the practical case, ref. [28] already has relatively large losses without considering the AM. The reason for this difference may be the same as previously analyzed, from the point of loss, the branch network of IEEE 33-bus system is better than the practical case. Therefore, the configuration of PV is not enough to increase the loss of IEEE 33-bus system. Based on the above analysis, we conclude, only from the PVHC calculation effect, that the method in ref. [28] is better. But, if the branch network and loss are considered, the method in this paper is more effective.

Table 15. Results of the different methods.

Methods		Ref. [28]			This Paper		
		PVHC (kWp)	Loss (kW)	Relaxation Deviation	PVHC (kWp)	Loss (kW)	Relaxation Deviation
IEEE 33-bussystem	No AM	11,362	137	10^{-14}	11,365	113	10^{-14}
	With AM	11,777	432	10^{-12}	11,420	112	10^{-13}
Practical case	No AM	7935	782	10^{-4}	6873	48	10^{-6}
	With AM	11,030	943	10^{-4}	10,189	167	10^{-9}

6. Conclusions

Calculating and improving the PVHC is conducive to the orderly development of the PV industry and the construction of green power grids. This paper presents a PVHC calculation model and improvement method considering the uncertainty of source load to achieve PVHC calculation as truly and accurately as possible. We have analyzed the effectiveness of the model by the IEEE 33-bus system and practical case, and then obtained the following conclusions:

(1) The established calculation model of PVHC can ensure that all the constraints are not exceeded, and the DN can operate safely and stably under the obtained PVHC;
(2) The PVHC is affected by the load and PV power generation efficiency. The smaller the load and the larger the PV power generation efficiency, the smaller the PVHC obtained;
(3) To shorten the power flow and alleviate the rise of voltage and current, the strategy of this paper is to first configure PV in each bus to absorb the load, and then configure PV in the bus closer to the balance bus for reverse power supply;
(4) SVC can improve the PVHC, but the effect is mediocre. For systems with poor branch networks, network reconfiguration can significantly increase PVHC by more than 50%.

In order to solve the problem of calculating the PVHC, this paper discusses the calculation method of PVHC by considering RTP and uncertainty and analyzes the AM methods to improve PVHC. The PVHC calculation model significantly guides the PV configuration of the distribution network. However, there are still many factors that are not taken into account in the model constructed in this paper. New modules in DN systems such as energy storage and EVs can increase the flexibility of the system and, thus, improve the PVHC. And, in the real world, various system faults will reduce the PVHC. If these are taken into account, the model will be more accurate. Moreover, due to ownership issues, the distributed system operator does not have access to individual PV installations, making the configuration of PV capacity not fully controllable, so the practical feasibility of the PVHC calculation model needs to be further investigated. In the future, we will add the energy storage and EVs models of DN system into the calculation model, and collect the faults that may occur in the DN system to make the results more accurate and reliable. In addition, we will further study the practical and feasible method for producing a PVHC calculation model.

Author Contributions: Conceptualization, T.L. and G.W.; methodology, Z.H.; software, G.W.; validation, T.L., G.W., S.L. and Z.H.; formal analysis, S.L.; investigation, T.L.; resources, T.L.; data curation, T.L.; writing—original draft preparation, H.H.; writing—review and editing, H.H.; visualization, T.L.; supervision, T.L. and Z.H.; project administration, Z.H.; funding acquisition, Z.H. All authors have read and agreed to the published version of the manuscript.

Funding: This research is funded by National Key R&D Program of China of 2022YFE0205300 and the Special Research Program of the Economic and Technology Research Institute of State Grid Fujian Electric Power Co., Ltd. of SGFJJY00GHJS2310137.

Informed Consent Statement: Informed consent was obtained from all subjects involved in the study.

Data Availability Statement: The original contributions presented in the study are included in the article, further inquiries can be directed to the corresponding author.

Acknowledgments: The authors would also like to thank the anonymous reviewers for their valuable comments and suggestions to improve the quality of the paper.

Conflicts of Interest: Authors Tingting Lin, Guilian Wu and Sudan Lai were employed by the companies State Grid Fujian Electric Power Co., Ltd. and Distribution Network Planning and Operation Control Technology in Multiple Disaster Superimposed Areas State Grid Corporation Laboratory, Ltd. The remaining authors declare that the research was conducted in the absence of any commercial or financial relationships that could be construed as a potential conflict of interest.

Nomenclature of Symbols and Abbreviations

Abbreviations	
PV	Photovoltaic
DN	Distribution Network
PVHC	Photovoltaic Hosting Capacity
MISOC	Mixed-Integer Second-Order Cone
RTP	Reverse Transmission Phenomenon
AM	Active Management
SVC	Static Var Compensators
PSO	Particle Swarm Optimization
GA	Genetic Algorithm
NSGA-II	Non-dominated Sorting Genetic Algorithm II
MOAGWO	Multi-Objective Advanced Gray Wolf Optimization
OLTC	On-Load-Tap-Changers regulation
SOP	Soft Open Point
EVs	Electric Vehicles
C&CG	Column-and-Constraint Generation
Sets	
I	Set of buses, indexed by i , and $I = \{1,2,\ldots,n_b\}$
J	Set of branches, indexed by j, and $J = \{1,2,\ldots,n_l\}$
S	Set of scenarios, indexed by s
$\Omega_{up,i}$	the branch set with bus i as the start bus
$\Omega_{down,i}$	the branch set with bus i as the end bus
Parameters	
$\varphi_{v,s}$	Actual PV power generation efficiency in scenario s
$\varphi'_{v,s}$	Predicted PV power generation efficiency in scenario s
$\Delta\varphi_{v+,s}$	Upward deviation value of PV power generation efficiency in scenario s
$\Delta\varphi_{v-,s}$	Downward deviation value of PV power generation efficiency in scenario s
$\alpha_{v+,s}$	Upward deviation coefficient of PV power generation efficiency in scenario s
$\alpha_{v-,s}$	Downward deviation coefficient of PV power generation efficiency in scenario s
$P_{v,i,s}$	PV power generation of scenario s and bus i
$P_{d,i,s}$	Actual load of scenario s and bus i
$P'_{d,i,s}$	Predicted load of scenario s and bus i
$\Delta P_{d+,i,s}$	Upward deviation value of load of scenario s and bus i
$\Delta P_{d-,i,s}$	Downward deviation value of load of scenario s and bus i
$\alpha_{d+,i,s}$	Upward deviation coefficient of load of scenario s and bus i
$\alpha_{d-,i,s}$	Downward deviation coefficient of load of scenario s and bus i
$P_{v,s}$	Total PV generation of all buses in scenario s
$P_{d,s}$	Total load of all buses in scenario s
$P_{loss,s}$	Total loss in scenario s
$P_{up,s}$	Power transmission from the DN to the upper power network in scenario s
S_v	PVHC
$\varphi_{vmax,s}$	The maximum PV power generation efficiency in scenario s
$P_{dmin,i,s}$	The minimum load of scenario s and bus i
$Q_{v,i,s}$	PV reactive power generation of scenario s and bus i
$Q_{d,i,s}$	Reactive load of scenario s and bus i
r_j	Resistance of branch j
x_j	Reactance of branch j

$Q_{up,s}$	Reactive power transmission from the DN to the upper power network in scenario s
V_{min}	Minimum voltage threshold
V_{max}	Maximum voltage threshold
I_{max}	Maximum current threshold
$P_{up,max}$	Maximum transmission power threshold
$S_{v,min}$	Minimum PV configuration capacity
$S_{v,max}$	Maximum PV configuration capacity
$\theta_{v,max}$	Maximum inverse angle
ϵ_g	Arbitrary number
ϵ_{min}	A minimal positive value close to zero
M	A maximal positive value
$V_{out,s}$	Overvoltage margin of scenario s
$I_{out,s}$	Overcurrent margin of scenario s
Variables	
$S_{v,i,s}$	PV configuration capacity of scenario s and bus i
$P_{j,s}$	Active power of scenario s and branch j
$Q_{j,s}$	Reactive power of scenario s and branch j
$I_{j,s}$	Current of scenario s and branch j
$V_{i,s}$	Voltage of scenario s and bus i
$\theta_{v,i,s}$	Inverse angle of scenario s and bus i
$F_{j,s}$	Virtual power of scenario s and branch j
$\alpha_{j,s}$	Branch switch status of scenario s and branch j
$I_{2,j,s}$	Square of current of scenario s and branch j
$V_{2,i,s}$	Square of voltage of scenario s and bus i

References

1. Poulek, V.; Aleš, Z.; Finsterle, T.; Libra, M.; Beránek, V.; Severová, L.; Belza, R.; Mrázek, J.; Kozelka, M.; Svoboda, R. Reliability characteristics of first-tier photovoltaic panels for agrivoltaic systems–practical consequences *Int. Agrophys.* **2024**, *38*, 383–391. [CrossRef] [PubMed]
2. Alturki, M.; Khodaei, A.; Paaso, A.; Bahramirad, S. Optimization-based distribution grid hosting capacity calculations. *Appl. Energy* **2018**, *219*, 350–360. [CrossRef]
3. Chathurangi, D.; Jayatunga, U.; Perera, S.; Agalgaonkar, A.; Siyambalapitiya, T. A nomographic tool to assess solar PV hosting capacity constrained by voltage rise in low-voltage distribution networks. *Int. J. Electr. Power Energy Syst.* **2022**, *134*, 107409. [CrossRef]
4. Shayani, R.A.; de Oliveira, M.A.G. Photovoltaic Generation Penetration Limits in Radial Distribution Systems. *IEEE Trans. Power Syst.* **2011**, *26*, 1625–1631. [CrossRef]
5. Alyami, S.; Wang, Y.; Wang, C.; Zhao, J.; Zhao, B. Adaptive Real Power Capping Method for Fair Overvoltage Regulation of Distribution Networks With High Penetration of PV Systems. *IEEE Trans. Smart Grid* **2014**, *5*, 2729–2738. [CrossRef]
6. Olivier, F.; Aristidou, P.; Ernst, D.; Van Cutsem, T. Active Management of Low-Voltage Networks for Mitigating Overvoltages Due to Photovoltaic Units. *IEEE Trans. Smart Grid* **2016**, *7*, 926–936. [CrossRef]
7. Georgilakis, P.S.; Hatziargyriou, N.D. Optimal Distributed Generation Placement in Power Distribution Networks: Models, Methods, and Future Research. *IEEE Trans. Power Syst.* **2013**, *28*, 3420–3428. [CrossRef]
8. Khodaei, A.; Shahidehpour, M. Microgrid-Based Co-Optimization of Generation and Transmission Planning in Power Systems. *IEEE Trans. Power Syst.* **2013**, *28*, 1582–1590. [CrossRef]
9. Wu, H.; Yuan, Y.; Zhang, X.; Miao, A.; Zhu, J. Robust comprehensive PV hosting capacity assessment model for active distribution networks with spatiotemporal correlation. *Appl. Energy* **2022**, *323*, 119558. [CrossRef]
10. Munikoti, S.; Abujubbeh, M.; Jhala, K.; Natarajan, B. A novel framework for hosting capacity analysis with spatio-temporal probabilistic voltage sensitivity analysis. *Int. J. Electr. Power Energy Syst.* **2022**, *134*, 107426. [CrossRef]
11. Zhao, L.; Feng, C.; Lu, Z.; Wang, Z.; Zhao, J.; Du, T. Evaluation of distribution network carrying capacity considering multi distributed resource access. In Proceedings of the 2022 IEEE 10th Joint International Information Technology and Artificial Intelligence Conference (ITAIC), Chongqing, China, 17–19 June 2022; Volume 10, pp. 328–332. [CrossRef]
12. Liu, X.; Ye, S.; Long, C.; Liu, L.; Li, D.; Li, H.; Pan, Y. Active Distribution Network Grid Expansion planning Technology Based on Power Grid Carrying Capacity Improvement. In Proceedings of the 2022 2nd International Conference on Intelligent Technology and Embedded Systems (ICITES), Chengdu, China, 23–26 September 2022; pp. 48–54. [CrossRef]
13. Zhao, Y.; Chen, F.; Li, Z.; Zhu, M.; Xie, T. Optimal dispatch of distribution network considering comprehensive carrying capacity. In Proceedings of the 2022 IEEE 10th Joint International Information Technology and Artificial Intelligence Conference (ITAIC), Chongqing, China, 17–19 June 2022; Volume 10, pp. 333–337. [CrossRef]

14. Zhang, X.; Zhang, Z.; Gong, X. Study on Consumption Capability of Large-Scale Photovoltaic Access to Regional Distribution Network. In Proceedings of the 2018 China International Conference on Electricity Distribution (CICED), Tianjin, China, 17–19 September 2018; pp. 2153–2157. [CrossRef]
15. Huangfu, X.; Li, Q.; Ding, Y.; Guo, Y.; Zhao, H.; Li, C.; Sun, D.; Wang, D.; Hou, X.; Fan, J. Evaluation Method of Distributed Photovoltaic Admission Capability Based on Voltage Sensitivity and Multi-Scenario Power Flow Simulation. In Proceedings of the 2022 IEEE 5th International Electrical and Energy Conference (CIEEC), Nanjing, China, 27–29 May 2022; pp. 257–262. [CrossRef]
16. Yu, H.; Li, K.; Guo, X.; Quan, S.; Zhao, H.; Zhu, X.; Li, C.; Zhu, W.; Yan, J.; Gao, K. Evaluation Method of Distributed Photovoltaic Carrying Capacity in Distribution Network Based on Voltage Sensitivity Ranking. In Proceedings of the 2022 IEEE 5th International Electrical and Energy Conference (CIEEC), Nanjing, China, 27–29 May 2022; pp. 238–243. [CrossRef]
17. Tao, Y.; Xu, M.; Zhang, J.; Tan, J.; Guo, Z.; Yuan, Z. Research on Calculation and Lifting Method of Distribution Network Hosting Capacity under High Permeability New Energy Access. In Proceedings of the 2022 IEEE 5th International Conference on Automation, Electronics and Electrical Engineering (AUTEEE), Shenyang, China, 18–20 November 2022; pp. 1002–1007. [CrossRef]
18. Gu, T.; Lv, Q.; Fan, Q.; Li, B.; Lin, C.; Zhang, H.; Mao, J. Two-stage distributionally robust assessment method for distributed PV hosting capacity of flexible distribution networks. *Energy Rep.* **2024**, *11*, 2266–2278. [CrossRef]
19. Mulenga, E.; Etherden, N. Multiple distribution networks hosting capacity assessment using a stochastic approach. *Sustain. Energy Grids Netw.* **2023**, *36*, 101170. [CrossRef]
20. Qammar, N.; Arshad, A.; Miller, R.J.; Mahmoud, K.; Lehtonen, M. Probabilistic hosting capacity assessment towards efficient PV-rich low-voltage distribution networks. *Electr. Power Syst. Res.* **2024**, *226*, 109940. [CrossRef]
21. Palacios-Garcia, E.J.; Moreno-Muñoz, A.; Santiago, I.; Moreno-Garcia, I.M.; Milanés-Montero, M.I. PV Hosting Capacity Analysis and Enhancement Using High Resolution Stochastic Modeling. *Energies* **2017**, *10*, 1488. [CrossRef]
22. Cho, Y.; Lee, E.; Baek, K.; Kim, J. Stochastic Optimization-Based hosting capacity estimation with volatile net load deviation in distribution grids. *Appl. Energy* **2023**, *341*, 121075. [CrossRef]
23. Ismael, S.M.; Abdel Aleem, S.H.; Abdelaziz, A.Y.; Zobaa, A.F. State-of-the-art of hosting capacity in modern power systems with distributed generation. *Renew. Energy* **2019**, *130*, 1002–1020. [CrossRef]
24. Jaramillo-Leon, B.; Zambrano-Asanza, S.; Franco, J.F.; Soares, J.; Leite, J.B. Allocation and smart inverter setting of ground-mounted photovoltaic power plants for the maximization of hosting capacity in distribution networks. *Renew. Energy* **2024**, *223*, 119968. [CrossRef]
25. Kazemi-Robati, E.; Sepasian, M.S.; Hafezi, H.; Arasteh, H. PV-hosting-capacity enhancement and power-quality improvement through multiobjective reconfiguration of harmonic-polluted distribution systems. *Int. J. Electr. Power Energy Syst.* **2022**, *140*, 107972. [CrossRef]
26. Ahmadi, B.; Ceylan, O.; Ozdemir, A. Reinforcement of the distribution grids to improve the hosting capacity of distributed generation: Multi-objective framework. *Electr. Power Syst. Res.* **2023**, *217*, 109120. [CrossRef]
27. Chen, X.; Wu, W.; Zhang, B. Robust Capacity Assessment of Distributed Generation in Unbalanced Distribution Networks Incorporating ANM Techniques. *IEEE Trans. Sustain. Energy* **2018**, *9*, 651–663. [CrossRef]
28. Zhang, S.; Fang, Y.; Zhang, H.; Cheng, H.; Wang, X. Maximum Hosting Capacity of Photovoltaic Generation in SOP-Based Power Distribution Network Integrated With Electric Vehicles. *IEEE Trans. Ind. Informatics* **2022**, *18*, 8213–8224. [CrossRef]
29. Solat, S.; Aminifar, F.; Shayanfar, H. Distributed generation hosting capacity in electric distribution network in the presence of correlated uncertainties. *IET Gener. Transm. Distrib.* **2020**, *15*, 836–848. [CrossRef]
30. Rabiee, A.; Mohseni-Bonab, S.M. Maximizing hosting capacity of renewable energy sources in distribution networks: A multi-objective and scenario-based approach. *Energy* **2017**, *120*, 417–430. [CrossRef]
31. Yao, H.; Qin, W.; Jing, X.; Zhu, Z.; Wang, K.; Han, X.; Wang, P. Possibilistic evaluation of photovoltaic hosting capacity on distribution networks under uncertain environment. *Appl. Energy* **2022**, *324*, 119681. [CrossRef]
32. Zou, Y.; Xu, Y.; Li, J. Aggregator-Network Coordinated Peer-to-Peer Multi-Energy Trading via Adaptive Robust Stochastic Optimization. *IEEE Trans. Power Syst.* **2024**, 1–13. [CrossRef]
33. Zheng, X.; Khodayar, M.E.; Wang, J.; Yue, M.; Zhou, A. Distributionally Robust Multistage Dispatch with Discrete Recourse of Energy Storage Systems. *IEEE Trans. Power Syst.* **2024**, 1–14. [CrossRef]
34. Lee, J.; Bérard, J.P.; Razeghi, G.; Samuelsen, S. Maximizing PV hosting capacity of distribution feeder microgrid. *Appl. Energy* **2020**, *261*, 114400. [CrossRef]
35. Xu, X.; Li, J.; Xu, Z.; Zhao, J.; Lai, C.S. Enhancing photovoltaic hosting capacity—A stochastic approach to optimal planning of static var compensator devices in distribution networks. *Appl. Energy* **2019**, *238*, 952–962. [CrossRef]
36. Lazo, J.; Watts, D. Stochastic model for active distribution networks planning: An analysis of the combination of active network management schemes. *Renew. Sustain. Energy Rev.* **2024**, *191*, 114156. [CrossRef]
37. Xiang, Y.; Dai, J.; Xue, P.; Liu, J. Autonomous topology planning for distribution network expansion: A learning-based decoupled optimization method. *Appl. Energy* **2023**, *348*, 121522. [CrossRef]
38. Mejia, M.A.; Macedo, L.H.; Muñoz-Delgado, G.; Contreras, J.; Padilha-Feltrin, A. Active distribution system planning considering non-utility-owned electric vehicle charging stations and network reconfiguration. *Sustain. Energy Grids Netw.* **2023**, *35*, 101101. [CrossRef]

39. Feizi, M.R.; Yin, S.; Khodayar, M.E. Solar photovoltaic dispatch margins with stochastic unbalanced demand in distribution networks. *Int. J. Electr. Power Energy Syst.* **2022**, *140*, 107976. [CrossRef]
40. Takenobu, Y.; Yasuda, N.; Minato, S-i.; Hayashi, Y. Scalable enumeration approach for maximizing hosting capacity of distributed generation. *Int. J. Electr. Power Energy Syst.* **2019**, *105*, 867–876. [CrossRef]
41. Albaker, A.; Alturki, M.; Abbassi, R.; Alqunun, K. Zonal-Based Optimal Microgrids Identification. *Energies* **2022**, *15*, 2446. [CrossRef]